

## **Nucleation of R-phase as studied by dynamic Young's modulus in the Ni<sub>49</sub>Ti<sub>51</sub> aged alloy**

B. Coluzzi, A. Biscarini, R. Campanella, G. Mazzolai and F.M. Mazzolai

*INFN-UDR of Perugia, Physics Department, University of Perugia, Via A. Pascoli 5, 06100 Perugia, Italy*

**Abstract.** The Young's modulus  $E$  and the internal friction  $Q^{-1}$  have been measured during thermal cycles carried out at temperatures higher than the start temperature  $R_s$  ( $R_s = 335$  K) of the B2→R martensitic transition in the Ni<sub>49</sub>Ti<sub>51</sub> alloy, prior cold-worked ( $\epsilon = 32$  %) and then aged at 673 K for 30 minutes. The cooling/heating  $E(T)$  and  $Q^{-1}(T)$  branches of cycles extending down to the temperatures 350, 340 and 336 K exhibit progressively increasing thermal hysteresis, while those referring to a cycle only extending down to 369 K does not. This thermal hysteresis is attributed to the formation of stable nuclei of R martensite at dislocation or at some other type of lattice defects.

### **1. INTRODUCTION**

Thermal hysteresis has been detected in the Young's modulus  $E(T)$  curves obtained during thermal cycling at temperatures higher than  $M_s$ , both in NiTi [1] and CuZnAl [2, 3] alloys. This hysteresis appears to be due neither to the early formation of surface martensite nor to lack of compositional homogeneity within the samples. The observed hysteresis has tentatively been attributed to the formation of stable martensite nuclei near "strong" lattice defects [4], the nature of which has not been identified so far. In the case of the CuZnAl system grain boundaries do not seem to play an essential role as the elastic hysteresis also occurs in single crystals [3].

For the NiTi system data exist on the Young's modulus hysteresis for the B2→B19' transition occurring in the solubilised and water quenched Ni-rich Ni<sub>50.8</sub>Ti<sub>49.2</sub> alloy, while no information is available for the B2→R transition, which takes place in deformed and aged NiTi alloys. Electron microscopy imaging experiments have shown that the R-phase can nucleate at single dislocations [5] and that the B2→R transition is preceded by the appearance of diffuse  $1/3\langle 110 \rangle$  reflections [6, 7]. Thus, it has appeared of interest to carry out accurate Young's modulus and internal friction (IF) measurements in temperature regions above the B2→R start-temperature  $R_s$ . The results of this investigation are reported in this note.

### **2. EXPERIMENTAL**

One specimen of nominal compositions 49 at. % Ni and 51 at.% Ti, in the following labelled sample F has been used in the present experiments. The specimen, prepared by CNR-Tempe, was in the shape of a rectangular bar, the dimensions of which are reported in Table 1, together with the thermo-mechanical treatments subsequently given to the sample. The coefficient of mechanical energy dissipation  $Q^{-1}$  and the Young's modulus  $E$  were derived from the resonance curve of free-free flexural vibration modes of the sample according to the standard anelastic techniques. The measurements were taken as a function of temperature at cooling/heating rates of about  $1.5 \cdot 10^{-2}$  K/s and at deformation amplitudes of the order of  $10^{-7}$ . The experimental set up used has been described in detail elsewhere [8].

**Table 1. Dimensions and thermo-mechanical treatments given to the specimen**

Alloy	Dimensions (mm <sup>3</sup> )	Treatment
Ni <sub>49</sub> Ti <sub>51</sub>	45.1x5.2x1.0	1. Cold-working at R.T ( $\epsilon = 32\%$ ) 2. Ageing at 673 K for 30 min 3. Quenching in water at R.T.

### 3. RESULTS

After treatment 3 of Table 1 sample F was submitted to a deep thermal measuring cycle (400→80→400 K) followed by a series of partial thermal cycles between an upper temperature  $T_H$  ( $T_H = 382$  K) and a gradually decreasing lower temperature  $T_L$  ( $T_L = 369, 350, 340$  and  $336$  K). After completion of all the thermal cycles the temperature dependence of the heat flow (DSC) was determined by using a sample cut from the F bar. The calorimetric data are plotted in figure 1 and the elastic/anelastic ones in figures from 2 to 4. As can be seen in figure 1 the direct and inverse transitions take place in two steps, the one at higher temperature corresponds to the  $B2 \leftrightarrow R$  transition, the other to the  $R \leftrightarrow B19'$  transition. It is worth noting that the DSC anomaly associated with the first transition is much wider than the one associated with the second and that a large hysteresis is displayed by both. The characteristic temperatures deduced from figure 1 by the base line method are:  $R_s = 335$  K,  $R_f = 330$  K,  $M_s = 314$  K,  $M_f = 286$  K for the direct transition and  $R'_s = 339$  K,  $R'_f = 352$  K,  $A'_s = 354$  and  $A'_f = 358$  K for the reverse one.

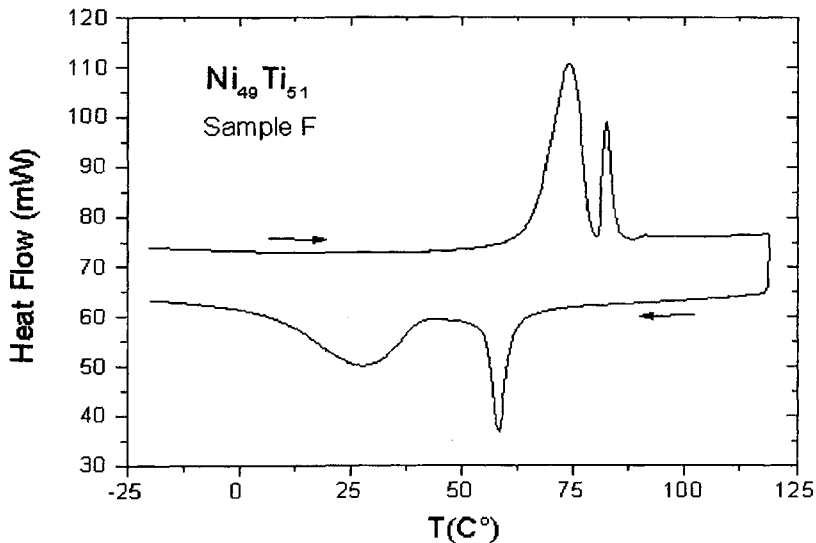


**Figure 1:** Temperature dependence of heat flow (DSC) as measured in a piececut from sample F at the end of all the Young's modulus and internal friction measurements. The data have been taken at 20 K/min

The overall temperature dependence of  $E$  and  $Q^{-1}$  is shown in figure 2, where are also marked the characteristic temperatures deduced from DSC data. As can be seen,  $E$  decreases on approaching  $R_s$  from high temperature. This elastic softening, as represented by the relative change  $\Delta E_{\text{soft}}/E_0$ , amounts to about -22% ( $\Delta E_{\text{soft}}/E_0 = (E(R_s) - E_0)/E_0$ ;  $E_0 = E(400)$ ) and is a precursor effect of the transition. The relative modulus change  $\Delta E_R/E_0$ , occurring between  $R_s$  and  $R_f$ , in the following denoted as "relative modulus defect", amounts to -31% and is expected to be due to the presence within the R martensite of mobile twin interfaces ( $\Delta E_R/E_0 = (E(R_s) - E(R_f))/E_0$ ) [12].

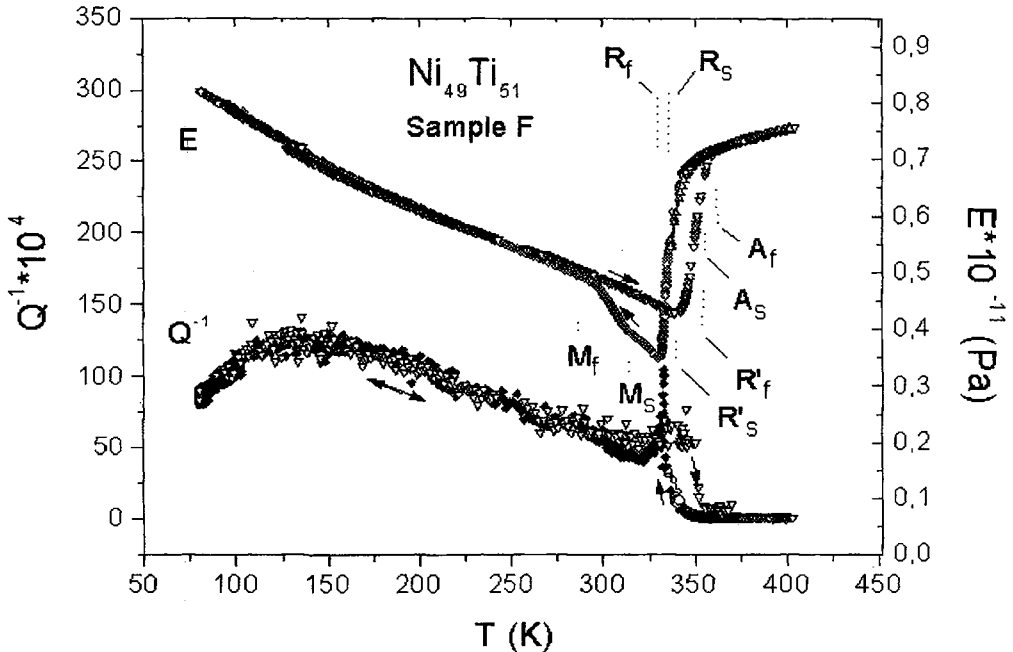


**Figure 2:** Young's modulus  $E$  and internal friction  $Q^{-1}$  measured during an initial complete temperature cycle. The characteristic temperatures of the direct ( $R_s$ ,  $M_s$ ) and reverse ( $R'_s$ ,  $A'_s$ )  $A \leftrightarrow R$  and  $R \leftrightarrow M$  transitions have been determined from data in figure 1

The energy dissipation coefficient  $Q^{-1}(T)$  is high in the B19' martensite and exhibits a well developed broad peak ( $P_{TWM}$ ) at around 130 K. The main features of the  $E(T)$  and  $Q^{-1}(T)$  curves in figure 1 appear to be common to prior deformed and then aged NiTi/NiTiCu alloys and have already been reported [9, 10] or will appear soon [11, 12], thus, here only the  $E(T)$  and  $Q^{-1}(T)$  behaviours above  $R_s$  will be discussed.

The results of the first two partial thermal cycles ( $T_L = 369$  and  $350$  K) are displayed in figure 3. Within the limit of the experimental accuracy the cooling/heating sets of  $E(T)$  data perfectly overlap one another in the first cycle; this applies to both cycles for the  $Q^{-1}(T)$  results. The  $E(T)$  measurements referring to the second cycle, on the contrary, show thermal hysteresis as the heating data are steadily lower than the cooling ones in the range 350-370 K. The  $E(T)$  and  $Q^{-1}(T)$  curves relative to one deeper cycle ( $T_L = 340$  K) is compared with the previous ones in figure 4. A more evident hysteretic loop is observed in the Young's modulus and also the  $Q^{-1}(T)$  data show thermal hysteresis.

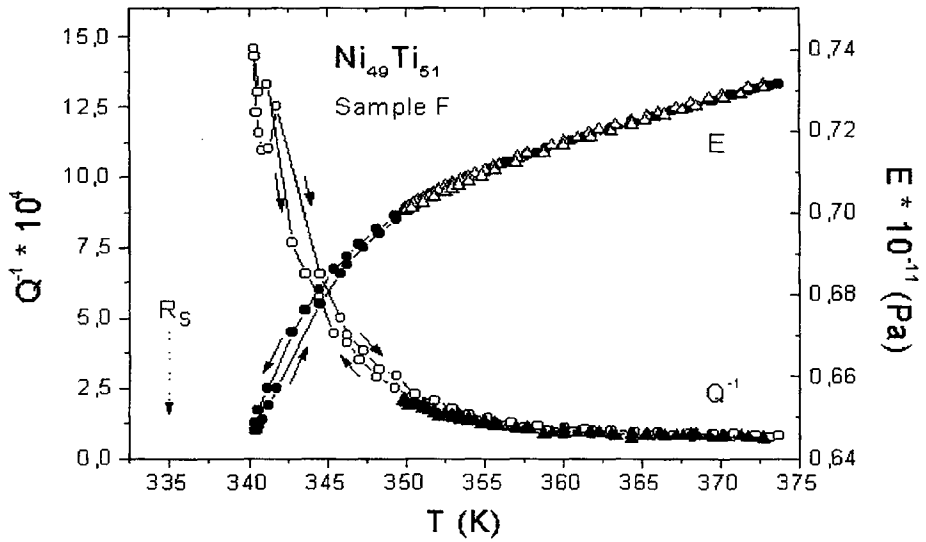


Figure 3: Temperature dependence of  $E$  and  $Q^{-1}$  during the first and second partial cooling/heating cycles. Complete overlapping is seen between the cooling and heating  $Q^{-1}$  data sets, while hysteresis is noted in the  $E(T)$  curves for the deeper cycle

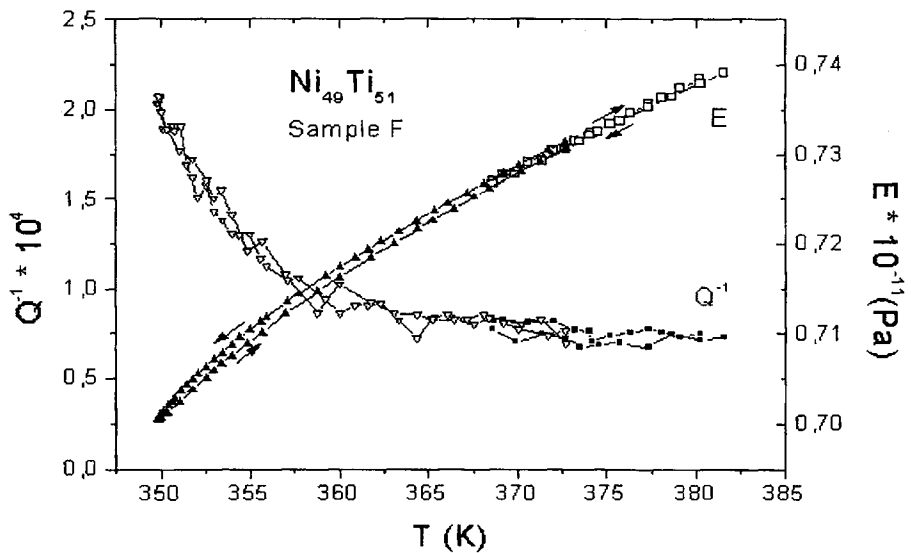
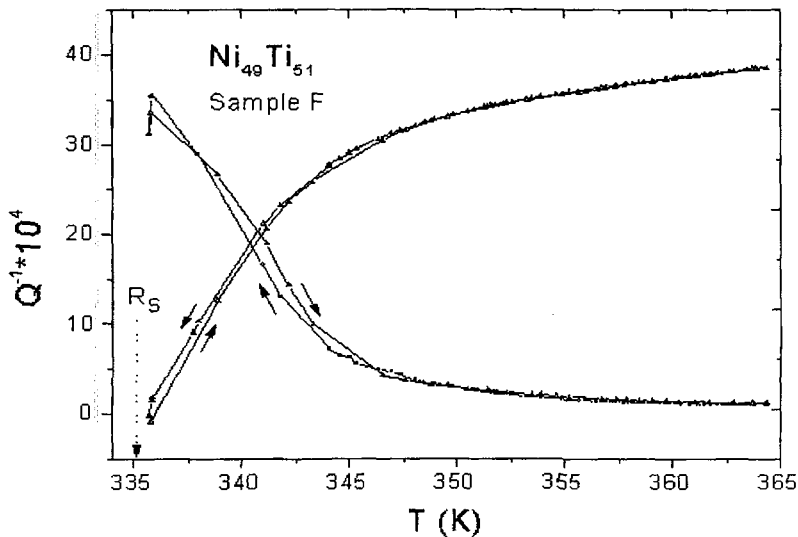


Figure 4: As in fig. 3 but for the third partial cycle. Thermal hysteresis is noted between the cooling and heating  $E(T)$  and  $Q^{-1}(T)$  data sets

In figure 5 are shown the results obtained with a further cycle, the lowest temperature of which ( $T_L = 336$  K) is only one degree higher than the start-temperature  $R_s$ . Thermal hysteresis is seen between 336 and 350 K, both in the  $E(T)$  and  $Q^{-1}(T)$  cooling/heating curves. Above 350 K for this cycle and above 369 K for the first one the cooling and heating curves perfectly overlap one another, thus excluding that the observed hysteresis may be an experimental artefact.



**Figure 5:** As in fig. 3 but for the fourth partial cycle. Thermal hysteresis is noted between the cooling and heating  $E(T)$  and  $Q^{-1}(T)$  data sets

#### 4. DISCUSSION AND CONCLUSIONS

The hysteresis exhibited by the Young's modulus and the internal friction over temperature regions above  $R_s$  indicates that some process precedes the actual  $B2 \rightarrow R$  transition. The present data show general similarities with the previous ones for the solubilised  $Ni_{50.8}Ti_{49.2}$  alloy [2]. Thus, we assume that the origin of the hysteresis is the same for the two alloys and is the formation (on cooling) and the delayed disappearance (on heating) of stable nuclei of martensite at "strong" lattice defects. Of course, differences in the nucleation sites, the inner structure of the nuclei and of the nucleus/matrix interfaces are conceivable.

The occurrence of various lattice modifications prior to the  $B2 \rightarrow R$  transformation in NiTi based alloys has been ascertained by diffraction experiments [5, 7, 13-16]. These modifications have recently been clarified a great deal. In particular, it has been established that the  $B2 \leftrightarrow R$  transition is displacive, first order and is preceded by the appearance of weak diffuse  $1/3 \langle 110 \rangle$  reflections [5, 7]. Furthermore, evidence has been provided that variants of the R martensite can nucleate at single dislocations on cooling [5, 7]. The nature of the  $1/3$  diffuse reflections, on the other hand, has not been identified so far.

Taking into account the above achievements as well as the high density of dislocations present in our pre-deformed sample, it would appear reasonable to associate the observed thermal hysteresis with the formation of stable nuclei of R martensite at dislocation sites. However, isolated dislocations are "weak" defects [4] and embryo stabilisation at such defects is, actually, not expected to occur. Thus, a possible self-consistent interpretation might be as follows: a) nucleation at dislocations is barrierless, that

is immediately followed by growth of the nucleus into macroscopic martensite platelets in keeping with calculations [4]; b) the embryo stabilisation takes place at defects other than dislocations (for example at coherent/semi-coherent  $Ti_2Ni$  precipitates). Alternatively, the data could be accounted for by assuming that: a) the short-distance stress fields of dislocations, not adequately taken into account in the calculations, play a crucial role; b) the embryo stabilisation occurs at dislocation cores. To discriminate between these two possibilities experiments in prior recrystallised and then aged samples would be needed. For the moment it suffices to realise that thermal elastic hysteresis besides the  $B2 \rightarrow B19'$  also accompanies the  $B2 \rightarrow R$  transition

The the question now arises about whether an interrelation may exist between the elastic thermal hysteresis and the weak diffuse  $1/3\langle 110 \rangle$  reflections. It is attempting to attribute both phenomena to the same mechanism and, because all the models presented so far for the diffraction data seem questionable [7], it is appealing to associate also the weak diffuse  $1/3\langle 110 \rangle$  reflections to the presence of stable nuclei having an inner structure similar to the one of the final R martensite.

### Acknowledgements

The authors gratefully acknowledge financial support from Progetto Strategico Materiali Speciali per Tecnologie Avanzate del CNR and dr. A. Tuissi for providing them with the sample

### References

1. B. Coluzzi, A. Biscarini, S. Piazza and F. M. Mazzolai, *J. Phys.*, **C8**, 397 (1996)
2. R. Campanella, B. Coluzzi, A. Biscarini, L. Trotta, G. Mazzolai and F. M. Mazzolai, *Scripta Mater.*, **41**, 1211 (1999)
3. G. Mazzolai, A. Biscarini, R. Campanella, B. Coluzzi and F. M. Mazzolai, *J. Alloys and Compounds*. In press
4. G. B. Olson and A. L. Roitburd, in *Martensite*, ed. by G. B. Olson and M. Cohen, ASM International, Materials Park, OH (1992)
5. T. Fukuda, T. Saburi, K. Doi and S. Nenno, *Mater. Trans JIM*, **33**, 271 (1992)
6. T. Saburi, in *Shape Memory Materials* ed. by K. Otsuka and C. M. Wayman, Cambridge University Press, 1998
7. T. Tamiya, D. Shindo, Y. Murakami, Y. Bando and T. Otsuka, *Mater. Trans. JIM*, **39**, 714 (1998)
8. B. Coluzzi, A. Biscarini and F. M. Mazzolai, *Rev. Sci. Instrum.*, **67**, 4240 (1996)
9. B. Coluzzi, A. Biscarini, R. Campanella, L. Trotta, G. Mazzolai, A. Tuissi and F. M. Mazzolai, *Acta Mater.*, **47**, 1965 (1999)
10. A. Biscarini, R. Campanella, B. Coluzzi, L. Di Masso, G. Mazzolai, and F. M. Mazzolai, *Proc. Internat. Conf. on Solid-Solid Phase Transf. '99*, ed. by M. Koiwa, K. Otsuka and T. Miyazaki, *JIM*, 1999
11. F. M. Mazzolai, A. Biscarini, R. Campanella, B. Coluzzi, G. Mazzolai and A. Rotini. Submitted to *Acta Mater.*
12. A. Rotini, A. Biscarini, R. Campanella, B. Coluzzi, G. Mazzolai, and F. M. Mazzolai. Submitted to *Scripta Mater.*
13. G.M. Michal, P. Moine and R. Sinclair, *Acta Metall.*, **30**, 125 (1982)
14. C. M. Hwang, M. Meichle, M. B. Salamon and C.M. Wayman, *Phil. Mag.*, **A47**, 9 and 31 (1983)
15. M. B. Salamon, M. Meichle and C. M. Wayman, *Phys. Rev.*, **B31**, 7306 (1985)
16. S. M. Shapiro, Y. Noda, Y. Fujjii and Y. Yamada, *Phys. Rev.*, **B30**, 4314 (1984)
17. T. Hara, T. Ohba, E. Okunishi and K. Otsuka, *Mater. Trans. JIM*, **38**, 11 (1997)